



LUND UNIVERSITY

3D processing and imaging of near field ISAR data in an arbitrary measurement geometry

Larsson, Christer; Erickson, Roland; Lunden, Olof

Published in:
AMTA Proceedings

1995

[Link to publication](#)

Citation for published version (APA):

Larsson, C., Erickson, R., & Lunden, O. (1995). 3D processing and imaging of near field ISAR data in an arbitrary measurement geometry. In *AMTA Proceedings* (Vol. 17, pp. 106-110). AMTA.

Total number of authors:
3

General rights

Unless other specific re-use rights are stated the following general rights apply:
Copyright and moral rights for the publications made accessible in the public portal are retained by the authors and/or other copyright owners and it is a condition of accessing publications that users recognise and abide by the legal requirements associated with these rights.

- Users may download and print one copy of any publication from the public portal for the purpose of private study or research.
- You may not further distribute the material or use it for any profit-making activity or commercial gain
- You may freely distribute the URL identifying the publication in the public portal

Read more about Creative commons licenses: <https://creativecommons.org/licenses/>

Take down policy

If you believe that this document breaches copyright please contact us providing details, and we will remove access to the work immediately and investigate your claim.

LUND UNIVERSITY

PO Box 117
221 00 Lund
+46 46-222 00 00

3D PROCESSING AND IMAGING OF NEAR FIELD ISAR DATA IN AN ARBITRARY MEASUREMENT GEOMETRY

Christer U.S. Larsson, Roland Erickson and Olof Lundén

National Defence Research Establishment, PO Box 1165, S-581 11 Linköping,
Sweden

ABSTRACT

Near field inverse synthetic aperture radar 3D imaging is performed utilizing data for arbitrary, but known, positioning of the target. The general imaging method was implemented and is described. This straightforward approach has many advantages. It gives geometrically correct images in near field. Field corrections can be applied independently for each frequency, antenna position and point of interest in the target volume. The main disadvantage is that the processing using the algorithm is very time consuming. However, in many cases it is only necessary to perform the analysis on a few cuts through the object volume.

Keywords: Radar Imaging, Spherical Near Field, RCS Measurements, 3D Imaging

1. INTRODUCTION

Two-dimensional radar cross section imaging has been shown to be a very useful analysis tool in applications such as signature reduction of existing platforms or on scale models at the design stage.

Imaging can be performed by calculation of a reflectivity density function, $g(\mathbf{r})$, for the points in the object plane using an inverse Fourier transform [1].

The measurement is done at n_f frequencies and at n_ϕ angles. We want to calculate $g(\mathbf{r})$ at n_x by n_y points in the object plane coordinate system. A solution of the Fourier integral numerically will then entail a summation over four indices with a total of $n_f \cdot n_\phi \cdot n_x \cdot n_y$ terms.

Using this general imaging method has many advantages. The method is correct for near field conditions, the measurement geometry can be chosen arbitrarily and no interpolation has to be performed in the processing. Corrections for an inhomogenous illuminating field, the r^4 dependency or other effects can be performed independently for each frequency, antenna position and point of interest in the target plane. Furthermore, $g(\mathbf{r})$ only has to be calculated for the desired object points.

The main disadvantage with the general imaging procedure is the high demand on computer time. If one or more of the advantages listed above are sacrificed the computer time can be reduced significantly in most cases by using the fast Fourier transform (FFT) and one- or two-dimensional interpolation. An example of such a method is to perform an FFT over the frequency sweep at each measurement angle. This is followed by a one-dimensional interpolation. This was implemented for 3D imaging by Scarborough *et al* in [2]. The described method reduces the computing time without restricting the measurement geometry or loss of data in interpolation processes. The only disadvantage is that the completely independent frequency dependent field corrections no longer can be performed.

By assuming far field conditions and doing a two-dimensional interpolation to a rectangular grid in the frequency-angle plane a two-dimensional FFT can be utilized. This reduces the summation to one over $n_x \cdot n_y \cdot (\log(n_f) + \log(n_\phi))$ terms. This method is what is usually referred to as conventional focused inverse synthetic aperture radar (ISAR). Close to real-time performance for 2D imaging can be obtained even in software based solutions. The technique can also be applied to three-dimensional imaging. This is studied by Flynn and Pressnall in [3]. They also consider triangulation methods using a limited number of elevation cuts for 3D imaging [3].

Results from 3D imaging are also reported in [4,5] without describing the method in detail.

Fast workstations have become common and it is now feasible to use the general imaging algorithm even for large data sets in two dimensions.

In fact, we will show here that general imaging is an attractive procedure even for three dimensional data acquisition and imaging. In three dimensions the measurement is performed for n_f frequencies at $n_\phi \cdot n_\theta$ angles and $g(\mathbf{r})$ is calculated for $n_x \cdot n_y \cdot n_z$ points. The summation is therefore done over $n_f \cdot n_\phi \cdot n_\theta \cdot n_x \cdot n_y \cdot n_z$ terms. The analysis we show fulfils the requirement that the CPU-time used for the imaging is comparable to the data-acquisition time.

2. IMAGING METHOD

The complex radar cross section (RCS) amplitude a is determined at a frequency f , and the antenna at position r' relative to the object coordinate system. The reflectivity density function $g(r)$ for the object coordinate $r(x, y, z)$ can then be calculated by integrating over the complex amplitudes using a conjugate phase filter [1] described in equation (1). In practice a measurement is limited in frequency and angle range so a tapered weighting filter w is introduced to reduce the side lobe levels in the processed image.

The area (volume) element dF is expanded for two (three) dimensions in polar coordinates in relation (2). dF is necessary to focus the image.

$$g(r) = \int a w \exp\left(i \frac{4\pi f}{c} (|r - r'|)\right) dF \quad (1)$$

$$\begin{aligned} \text{2D: } a &= a(f, \varphi), w = w(f, \varphi), dF = f df d\varphi \\ \text{3D: } a &= a(f, \varphi, \theta), w = w(f, \varphi, \theta), \\ dF &= f^2 \cos(\theta) df d\varphi d\theta \end{aligned} \quad (2)$$

The extension to a measurement with data acquisition at discrete frequencies f_i and angles φ_j and θ_k is given in equation (3).

For the measurements that are described in this paper the frequency step is constant over the entire range. This is not necessary for the algorithms but it reduces the time necessary for computing with an order of magnitude.

The area (volume) elements for two (three) dimensional imaging are given in (4).

A Hanning window was used for the filtering.

$$g(r) = \sum_i \sum_j \sum_k a_{ijk} w_{ijk} \exp\left(i \frac{4\pi f_i}{c} (|r - r_{jk}'|)\right) \Delta F_{ijk} \quad (3)$$

$$\begin{aligned} \text{2D: } \Delta F_{ij} &= f_i \Delta f_i \Delta \varphi_j \\ \text{3D: } \Delta F_{ijk} &= f_i^2 \cos(\theta_k) \Delta f_i \Delta \varphi_j \Delta \theta_k \end{aligned} \quad (4)$$

3. EXPERIMENTAL

The experimental set up is shown in figure 1. The spherical field is incident from the left. The object is supported by a styrofoam mast which is mounted on a three-axis positioner. An absorbing screen is located to prevent that the incoming field illuminates the positioner

or the steel mast.

The experiment was performed in an anechoic chamber using a hardware gated system. The experimental parameters are given in Table 1.

Note that the total number of measurement points was 5871041 and the corresponding long measurement time.

4. 2D IMAGING RESULTS

Since the full three-dimensional processing is very time consuming it is essential to keep the number of processed cuts through the target volume down to a minimum. For this purpose it is useful to start the analysis by examining two dimensionally resolved images in both the horizontal and the vertical plane. The images shown in Figs. 2 and 3 were processed with a limited part of the data corresponding to elevation angle zero and azimuth angle zero, respectively.

It is evident from those two figures that most of the information is contained between vertical cross-range values -0.25 and +0.20 m. The three dimensional processing described in the next section was therefore done for cuts in this range.

Table 1: Experimental Parameters

Parameter	Value
Range	25 m
Elevation angle (θ)	15° - +15° with 0.25° steps
Azimuth angle (φ)	15° - +15° with 0.25° steps
Frequency	6.0 - 16.0 GHz with 25 MHz steps
Polarization	HH
Total Measurement Time	105 h

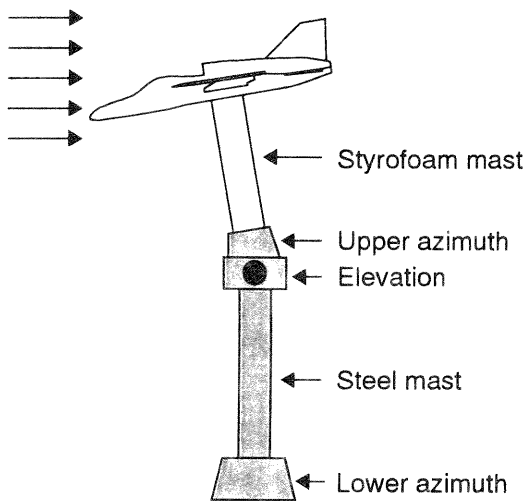


Figure 1. Experimental Set-Up

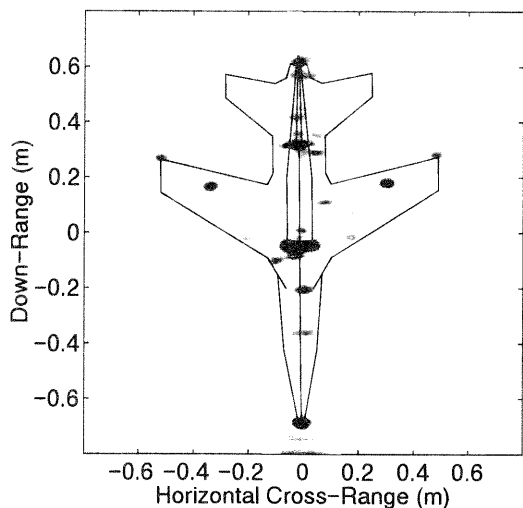


Figure 2. Two Dimensional ISAR Image of the Horizontal Plane.

5. 3D IMAGING RESULTS

Figs. 4 - 8 show results after processing for cuts at vertical cross-range = -0.20, -0.15, -0.10, -0.05 and 0.05 m. Figs. 9 and 10 show cuts through the vertical plane at horizontal cross-range = 0 and 0.09 m.

It is possible to use these cuts to find the position of reflection centers with an accuracy of a few centimeters. The scattering from a small auxiliary air inlet can be used

as an example. It can be found in the horizontal plane in figure 5 located to the right of the overlay main air inlet. Figure 10 is used to locate it in the vertical cross range where it is found below the overlay wing.

For this rather simple example with only a few scattering centers it would be possible to extract almost all information from a few 2D scans. However, for a more realistic, and complex, target the full 3D measurement and analysis will most likely prove necessary.

The presentation is problematic for 3D images. Using a 3D visualization system with the possibilities to rotate, zoom and so on it is easy to obtain all the needed information. This is not the case for paper images. Several cuts through the target volume are needed for an accurate description of the imaged object. One way would be to show consecutive cuts as a movie.

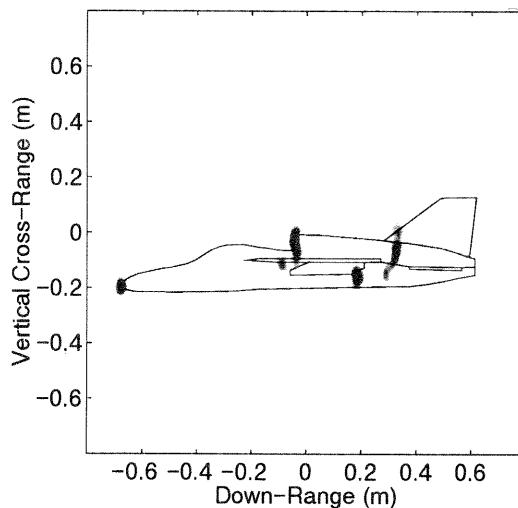


Figure 3. Two Dimensional ISAR Image of the Vertical Plane.

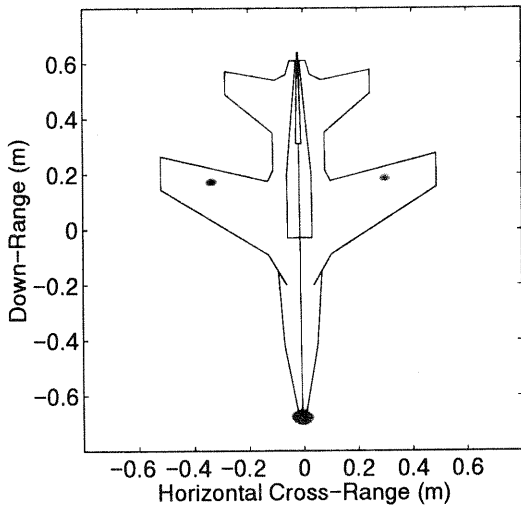


Figure 4. Three Dimensional ISAR.
Horizontal Cut at Vertical Cross-Range = -0.20 m

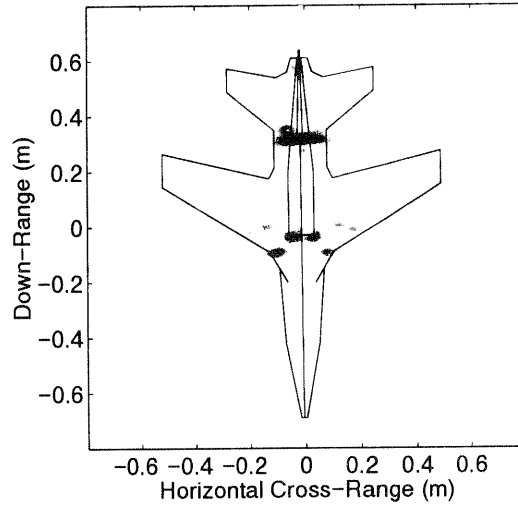


Figure 6. Three Dimensional ISAR.
Horizontal Cut at Vertical Cross-Range = -0.10 m

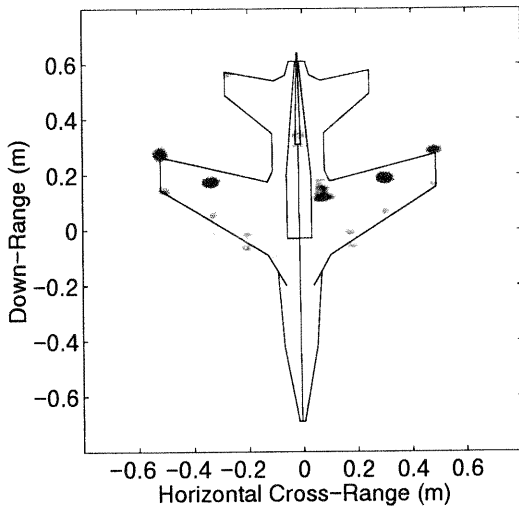


Figure 5. Three Dimensional ISAR.
Horizontal Cut at Vertical Cross-Range = -0.15 m

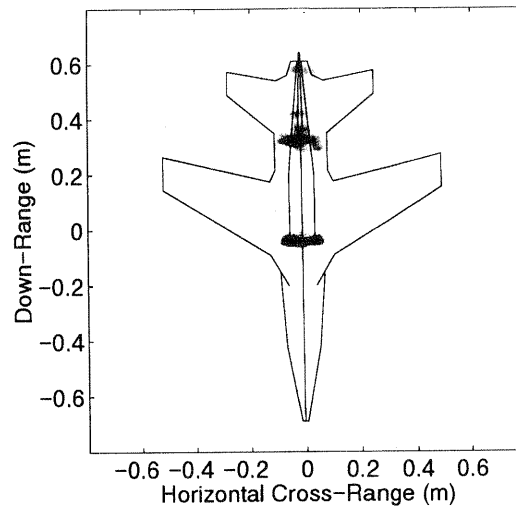


Figure 7. Three Dimensional ISAR.
Horizontal Cut at Vertical Cross-Range = -0.05 m

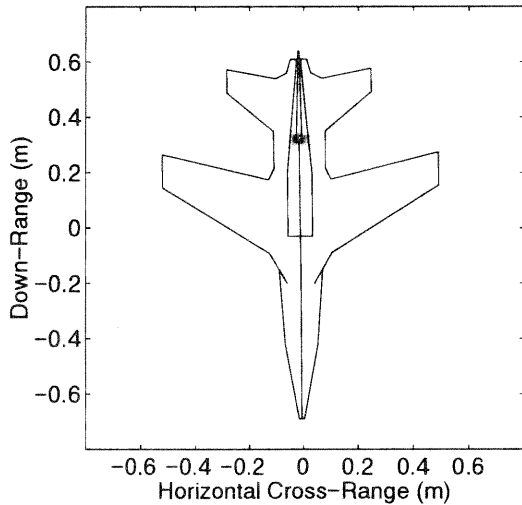


Figure 8. Three Dimensional ISAR.
Horizontal Cut at Vertical Cross-Range = 0.05 m

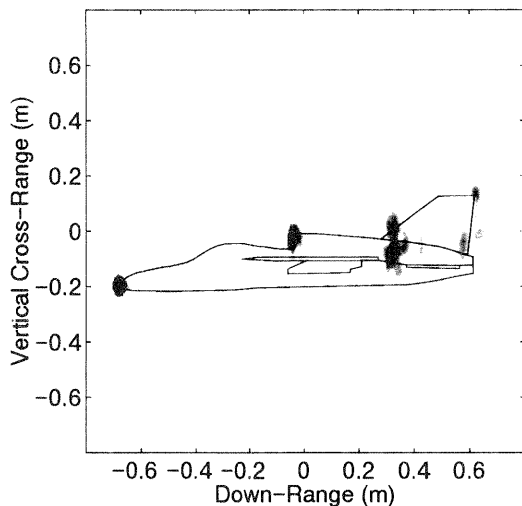


Figure 9. Three Dimensional ISAR.
Vertical Cut at Horizontal Cross-Range = 0.0 m

6. SUMMARY

We have shown that a relatively slow data acquisition system can be used for high resolution three dimensional ISAR imaging. The used algorithms are slow but general and therefore very flexible. This eliminates the restrictions on the measurement geometry and illuminating field that are necessary if faster algorithms are to be used. The implementation is straightforward for most geometries.

The long processing times that the general algorithms suffer from will be alleviated as long as computer technology continues to evolve.

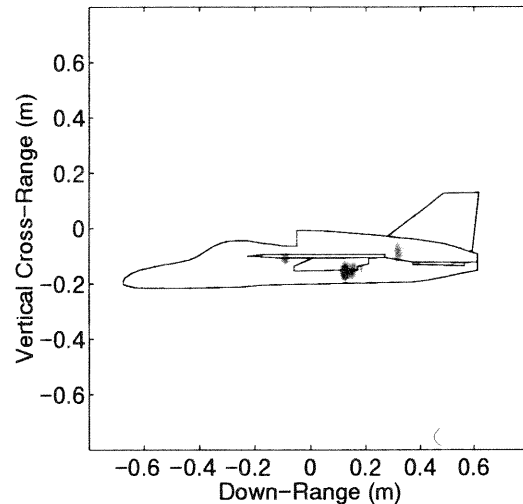


Figure 10. Three Dimensional ISAR.
Vertical Cut at Horizontal Cross-Range = 0.09 m

REFERENCES

- [1] D.L. Mensa, *High Resolution Radar Cross-Section Imaging*, Boston, Artech House, 1991.
- [2] S. Scarborough, C. Frost and S. Blejer, "A High Resolution Imaging Radar For Ground-Based Diagnostic Applications", AMTA 1994 p 468-473.
- [3] D. Flynn and S. Pressnall, "Practical Aspects of 3D Imaging", AMTA 1994, p 437-442.
- [4] G.B. Melson and D.R. Vanderpool, "A Portable 3D SAR RCS Imaging System", AMTA 1992, p 6-17 - 6-21.
- [5] R.L. Harris, B.E. Freburger, M.E. Lewis and C.F. Zappala, "Three-dimensional Radar Cross Section Imaging", AMTA 1994, p 443-448.